Electron Trapping in Self-Modulated Laser Wakefields by Raman Backscatter

C. I. Moore,* A. Ting, K. Krushelnick,† E. Esarey, R. F. Hubbard, B. Hafizi,‡ H. R. Burris, C. Manka,§ and P. Sprangle
Beam Physics Branch, Plasma Physics Division, Naval Research Laboratory, Washington, D.C. 20375
(Received 2 April 1997)

Simultaneous measurements of high energy electrons and plasma-wave characteristics have been conducted in a self-modulated laser-wakefield accelerator. Approximately 10^8 electrons were accelerated from the background plasma to energies greater than 1 MeV with a peak energy of approximately 30 MeV. A strong correlation between the plasma-wave amplitude and electron production was measured with no evidence of wave breaking. Simulations indicate plasma electrons are trapped by the low-phase-velocity beat waves produced by backward Raman scattering. [S0031-9007(97)04539-0]

PACS numbers: 41.75.Lx, 52.40.Nk, 52.75.Di

Conventional particle acceleration techniques are approaching fundamental limits to the accelerating fields due to material breakdown thresholds. New "structureless" techniques are now being investigated to overcome breakdown limitations [1]. Some of these techniques are vacuum laser accelerators [2], plasma beat-wave accelerators [3,4], and laser-wakefield accelerators [3,5]. We are currently investigating the self-modulated laser-wakefield accelerator (SM-LWFA) concept [6–10], in which a high power laser with a pulse length much longer than the plasma period, $2\pi/\omega_p$—where ω_p is the plasma frequency, is tightly focused in a plasma. A self-modulation instability, caused by relativistic self-focusing (RSF) and the forward stimulated Raman scattering (SRS) instability, breaks the laser pulse into beamlets of length $2\pi/\omega_p$ [10] which resonantly drive a large amplitude wakefield plasma wave. The plasma wave has a phase velocity v_p near the speed of light c and is well suited for high energy particle acceleration. RSF occurs when the laser power exceeds a critical power, $P_{\mathrm{RSF}} = 17(\omega_0/\omega_p)^2$ GW, where ω_0 is the laser frequency. The RSF threshold can be achieved with current laser technology in relatively high-density plasmas ($n_0 \sim 10^{19}$ cm^{-3}, $P_{\mathrm{RSF}} \sim 2$ TW). High-density plasmas can support large accelerating fields ($\sim$100 GV/m) before the onset of wave breaking. One-dimensional (1D) cold fluid theory [11] indicates that wave breaking occurs at an electric field amplitude of $E_{\mathrm{WB}} = \sqrt{2(\gamma_p - 1)}\,E_0$, where $\gamma_p = 1/\sqrt{1 - v_p^2/c^2}$ and $E_0 = mc\omega_p/e \approx 96\sqrt{n_0[\mathrm{cm}^{-3}]}$ V/m. Typically, $\gamma_p \approx \omega_0/\omega_p$, e.g., $\gamma_p \sim 10$ and $E_0 \sim 300$ GV/m for $n_0 \sim 10^{19}$ cm^{-3}.

Recent experiments have demonstrated electron acceleration in the SM-LWFA regime [7,8]. Experiments at Rutherford Appleton Laboratory [8] have achieved background plasma electron acceleration up to energies of 100 MeV using a laser power of 25 TW. The production of high energy electrons was observed to correlate with a spectral broadening of the forward SRS radiation. This broadening was attributed to the destruction of plasma-wave coherence due to wave breaking. Wave breaking was used as the explanation for the trapping and acceleration of background electrons by the plasma wave to the high energies observed.

The experiment at the Naval Research Laboratory (NRL) was also conducted in the SM-LWFA regime. However, much lower laser power was used (2.5 TW) and no evidence of wave breaking was apparent, although high energy electrons (up to 30 MeV) were observed. The experiment used the laser pulse from the NRL chirped pulse amplification laser system focused in a supersonic helium gas jet to generate large amplitude plasma waves. The 1054 nm laser pulse had a typical peak power of 2.5 TW (400 fs and 1 J) and was focused with a 15 cm focal length off-axis parabolic mirror to a vacuum spot radius of 6 μm ($I_{\mathrm{peak}} = 5 \times 10^{18}$ W/cm^2). The gas jet used a supersonic 3 mm diameter nozzle and produced a plasma density of 1.4×10^{19} cm^{-3} ($P_{\mathrm{RSF}} = 1.2$ TW) in fully ionized helium. The gas jet density profile was an approximately 2 mm flat top with 0.5 mm boundaries.

An electron spectrometer was used to measure the accelerated electron distribution. The spectrometer consisted of an electromagnet placed 10 cm after the plasma acceleration region and a $\frac{1}{2}$ in. thick plastic scintillator directly coupled to a photomultiplier tube (PMT) 15 cm after the magnet. The magnet and scintillator/PMT were aligned with the laser axis. Electrons with energies below a cutoff value, determined by the magnetic field of the electromagnet, were directed away from the laser axis and therefore the scintillator/PMT. This "inline" configuration resulted in measurement of the integrated number of electrons above the cutoff energy. Variation of the magnetic field determined the energy distribution of the accelerated electrons.

The magnet was a 45° sector magnet with a 2.5 mm gap, a field region 5.5 cm long, and a maximum field of 2.5 kG. Two graphite slabs separated by a 2 mm gap were placed over the input side of the magnet to limit the acceptance of the magnet to a 2 mm by 2.5 mm opening and therefore limit the electrons to a well defined path through the magnetic field. Four in. thick lead shielding was placed after the magnet to limit the acceptance of the scintillator/PMT

to electrons deflected between 0° and 8°. Two in. thick graphite was placed over the lead shielding to minimize x-ray production from deflected electrons. The length of the magnetic field region, the magnetic field strength, and the acceptance angle of the scintillator/PMT were used to calculate the energy calibration of the spectrometer. This method results in an energy determination which is accurate to approximately $-5\%/+25\%$. The main source of error in the calculated calibration is the omission of the magnet's fringe fields which causes up to a 20% underestimate of the electron energy. The measured electron energies are therefore the minimum electron energy, and actual electron energies are likely to be higher. The total relative number of electrons detected at a variety of cutoff energies and for multiple laser shots is shown in Fig. 1. The dashed line represents a signal-to-noise level of approximately two. Any signal above this level is a definitive electron detection. Electrons up to an energy of 28.5 MeV were clearly observed. The large fluctuations are shot-to-shot fluctuations which are most likely due to the strong nonlinearity of the laser-plasma interaction and the electron trapping mechanism. Measurement of the continuous electron energy spectrum from 500 keV to 5 MeV using film showed a smoothly monotonically decreasing electron energy distribution on each laser shot.

Measurement of the peak electron energy allows determination of a lower bound on the electric field of the wake. The laser was observed to be self-guided through a plasma over the full width of the 3 mm gas jet [12]. The acceleration distance is therefore the shorter of the plasma length or the dephasing distance [1], $L_d \approx \gamma_p^2 2\pi c/\omega_p$, which is the maximum distance a particle can be accelerated before slipping out of phase from the plasma wave. In our experiment, $L_d \approx 640\ \mu$m. The minimum accelerating field necessary to generate the highest energy electrons observed was therefore 47 GeV/m.

The absolute number of electrons accelerated above 1 MeV was also measured. For this measurement, the spectrometer cutoff energy was set to 1 MeV and the scintillator/PMT was replaced with a silicon surface barrier detector (SBD) with a detection area of 150 mm^2. The SBD consists of a 500 μm thick disk of high purity silicon set between two metallic plates which are biased at 200 V. High energy particles traveling through the silicon excited one electron-hole pair for every 3.6 eV of energy deposited in the silicon. Each electron incident on the SBD (1–30 MeV) passed completely through the SBD and deposited approximately 400 keV of energy, i.e., created 1.1×10^5 electron-hole pairs. The maximum number of electron-hole pairs created was measured to be 1×10^{11}. The number of electrons passing through the SBD was therefore approximately 10^6.

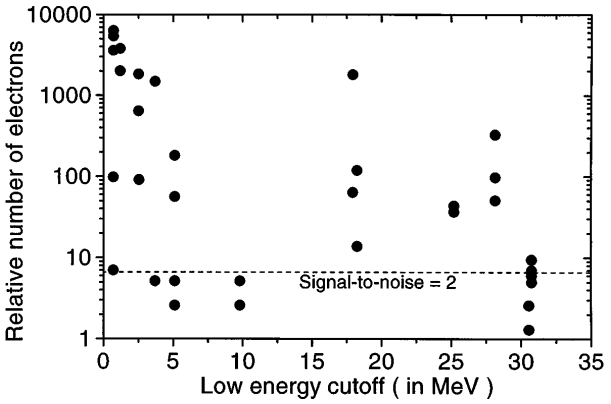

FIG. 1. Electron energy distribution measured with the scintillator and PMT. The dashed line represents a signal-to-noise level of approximately two. Any signal above this level is a clearly discernible electron peak.

The number of electrons measured by the SBD is only a small fraction of the electrons accelerated above 1 MeV due to the small acceptance angle of the magnet. In order to determine the fraction of electrons entering the magnet, the electron beam profile was measured using Kodak DEF x-ray film. The film showed a circular electron distribution centered on the laser axis with a cone angle approximately one-half the cone angle of the laser. Comparing the electron beam profile with the acceptance angle of the magnet showed that only 1% of the electrons were detected with the SBD. The total number of electrons accelerated above 1 MeV was therefore approximately 10^8.

The laser-plasma interaction was investigated by examining the SRS light generated during wakefield production which consequentially is related to the wakefield amplitude. For large amplitude plasma waves, nonlinear steepening results in harmonics $(\omega_0 \pm n\omega_p)$ of the standard SRS spectrum $(\omega_0 \pm \omega_p)$ [13]. SRS light was examined by placing a lens with an acceptance angle of $\pm 10°$ at 0°, 20°, 30°, 40°, 60°, and 90° to the laser axis to image anti-Stokes light into a 0.25 m spectrometer. The spectrometer measured the scattered spectrum from approximately 700 to 1000 nm which allowed the first four harmonics of the anti-Stokes line to be measured on each laser shot. The anti-Stokes spectra from 0°–60° were qualitatively similar with multiple orders and no broadening of the anti-Stokes peaks apparent. No anti-Stokes signal was observed at 90°. The angle of 40° was found empirically to provide the highest signal-to-noise ratio measurement of the SRS light and therefore the wakefield amplitude. Figure 2 shows a typical spectrum at 40° where up to the 4th harmonic is visible. The 5th harmonic was also measured on many shots by lowering the central wavelength of the spectrometer. The large angular spread of the anti-Stokes light is most likely due to the highly three-dimensional nature of the wakefield due to the tight focusing of the laser pulse (focal spot size ~ plasma wavelength) [14,15]. The multiple orders of SRS observed and their comparable intensities indicate that a highly nonlinear, large amplitude plasma wave was present. The nonlinearity of the plasma wave was correlated with the high energy electron production (see Fig. 2, inset), where the intensity of the 2nd harmonic exhibited a strong correlation with the

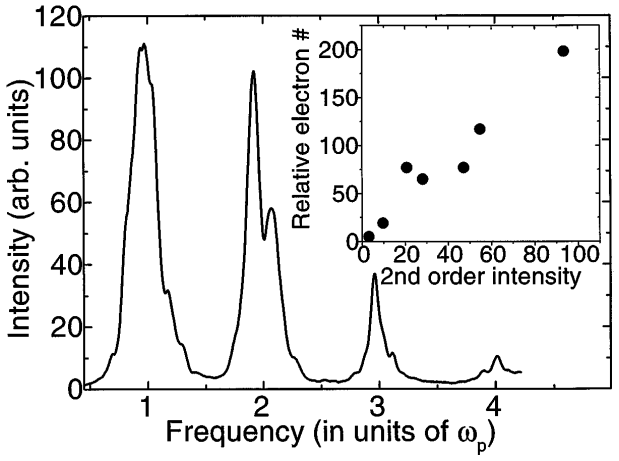

FIG. 2. The multiple order anti-Stokes spectrum. The well defined peaks show a highly nonlinear and coherent plasma wave with no evidence of wave breaking. The inset shows the relationship between the 2nd harmonic intensity and the number of electrons accelerated above 1 MeV.

number of accelerated electrons. In no instance during the experiment was any broadening of the scattered peaks observed. For example, the width of the 1st harmonic shown in Fig. 2, when the plasma wave was highly nonlinear, remained the same at the lower laser powers when the plasma wave remained linear. This indicates that the plasma waves were highly coherent with no evidence of wave breaking. Large shot-to-shot fluctuations were observed in the SRS spectrum concurrent with energetic electron production. The SRS spectrum and electron production fluctuations did not correlate with laser power, gas jet density, or any other directly controllable experimental parameter, except that for very low laser power (<1 TW) or low plasma density ($<10^{19}$ cm^{-3}) high energy electrons were never produced.

The generation of high energy electrons in this experiment without evidence for wave breaking strongly suggests that electrons are preaccelerated prior to being trapped by the wakefield. Previous experiments on our system have shown that approximately 10% of the incident laser pulse is reflected by backward Raman scattering (BRS) [16]. One candidate for preaccelerating electrons is the low phase velocity waves generated in BRS [17]. BRS produces backward traveling light of frequency $\omega_0 - \Delta\omega$, where $\omega_0 \gg \Delta\omega \geq \omega_p$. The BRS light wave can beat with the main laser pulse to generate a low phase velocity, $v_{\rm pb} = c\beta_{\rm pb} \approx (\Delta\omega/2\omega_0)c$, forward traveling electromagnetic beat wave. At high laser intensities, BRS occurs in the strong-pump limit, and the effects of the space-charge wave can be neglected [18]. The low phase velocity beat wave can pick up some of the low energy electrons in the background plasma and accelerate them to sufficient energies so as to be trapped by the high phase velocity wakefield ($v_p \approx c$). These trapped electrons can then be accelerated to much higher energies by the wakefield.

A 1D numerical simulation of this two stage acceleration mechanism shows the qualitative behavior observed in the experiment. The simulation prescribes three analytical wave potentials (normalized to mc^2/e) corresponding to the primary laser pulse a_0, the wakefield plasma wave ϕ, and the BRS electromagnetic wave a_1, and then pushes test particles in these potentials. The simulation uses the coordinates $\zeta = z - ct$ and $\tau = t$, the potentials are initialized in the region $\zeta \leq 0$ ($\zeta = 0$ corresponds to the initial front of the laser pulse), and the particles are initialized at rest in the region $\zeta > 0$.

The laser pulse parameters used in the simulation were chosen to closely model the experimental laser pulse parameters—peak normalized amplitude $a_{0m} = 1.4$, wavelength $\lambda = 1$ μm, and normalized frequency $\omega_0/\omega_p = 8.5$. The BRS is assumed to saturate at a normalized amplitude of $a_{1m} = 0.033$, based on analytical estimates for saturation in the strong-pump regime [18]. All potentials have a characteristic rise length of $\tau_r = 25/\omega_p$. Figure 3 plots the normalized axial momentum, $u_z = \gamma\beta_z = p_z/mc$, of simulation electrons at a wakefield potential of $\phi_0 = 0.6$ as a function of the coordinate ζ after 250 μm of propagation. This demonstrates the initial trapping of particles in the combined wake and BRS fields.

Production of energetic electrons is seen in the simulations only when the wakefield ϕ_0 and BRS a_1 amplitudes are sufficiently large. Figure 4 plots the peak electron energy, $W_{\rm max}$, and percentage, $f_{\rm tr}$, of plasma electrons which are trapped and accelerated to energies exceeding 10 MeV as a function of ϕ_0 after propagating 2.5 mm (other parameters are as in Fig. 3). The threshold for trapping is at $\phi_0 = 0.55$, beyond which $f_{\rm tr}$ rapidly increases. Once trapping occurs, $W_{\rm max}$ corresponds to the detuning limit,

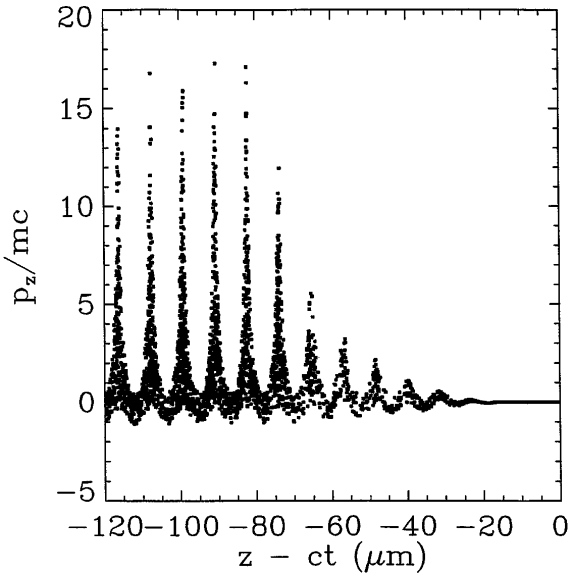

FIG. 3. Momentum phase space plot of the test electrons in the simulation after propagating $c\tau = 250$ μm with $a_0 = 1.4$, $a_1 = 0.033$, $\phi_0 = 0.6$, and $\omega_0/\omega_p = 8.5$. The laser pulse resides in the region $z - ct < 0$ and propagates to the right.

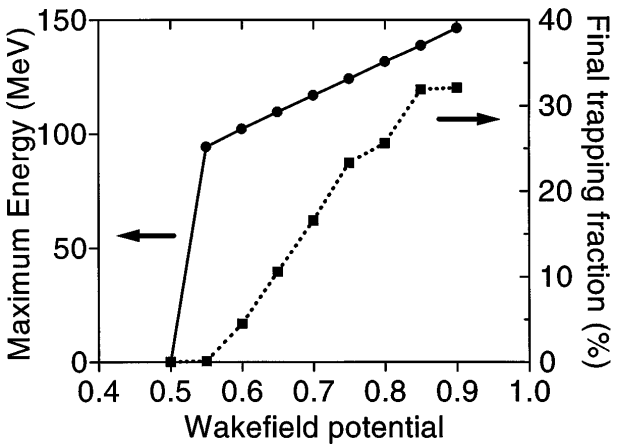

FIG. 4. Simulation results showing the maximum energy (solid line) and fraction above 10 MeV (dashed line) of accelerated electrons as a function of the wakefield potential ϕ_0 at $c\tau = 2.5$ mm for the parameters of Fig. 3. The y axis is in units of MeV for the energy and the percentage for the fraction.

i.e., $W_{\max} \approx 4\gamma_p^2 \phi_0 mc^2$. This is in qualitative agreement with the strong correlation of wakefield amplitude to high energy electron production observed in the experiments (see Fig. 2, inset).

An estimate for the trapping threshold can be obtained by requiring that the wakefield separatrix overlap the beat wave separatrix [1,19]. In momentum phase space (u_z versus $z - v_p t$), the minimum of the wakefield separatrix is given by $u_{w,\min} \approx \gamma_\perp^2/4\phi_0 - \phi_0$, assuming $2\phi_0\gamma_p/\gamma_\perp \gg 1$ where $\gamma_\perp = \sqrt{1 + a_0^2}$. Likewise, the maximum of the beat wave separatrix is given by $u_{b,\max} \approx \beta_{pb}\gamma_\perp + 2\sqrt{a_0 a_1}$. Passing of electrons from the slow beat wave to the fast wakefield can occur when $u_{b,\max} \geq u_{w,\min}$, i.e., $\phi_0 \geq (\gamma_\perp - u_{b,\max})/2$. This condition gives $\phi_0 \geq 0.6$ for the parameters of Fig. 3 ($\beta_{pb} = 0.059$, $a_0 = 1.4$, and $a_1 = 0.033$). A more accurate calculation gives a trapping threshold of $\phi_0 \geq 0.54$, in excellent agreement with the simulation results. Hence, self-trapping of plasma electrons can occur when $\phi_0 < 1$, i.e., well below the theoretical wave breaking amplitude of $\phi_0 = E_{\mathrm{WB}}/E_0 \approx 4$.

In conclusion, we have observed very high energy electrons (up to 30 MeV) accelerated in a SM-LWFA at relatively low laser power (2.5 TW). Optical diagnostics show the existence of highly nonlinear, large amplitude plasma waves. Using the dephasing distance as the acceleration length, the acceleration gradient is estimated to be greater than 47 GeV/m. The high energy electrons are observed with no sign of wave breaking. Numerical simulations show that low phase velocity beat waves generated by BRS can preaccelerate background plasma electrons to sufficient energy to be trapped by the high phase velocity wakefield. Both the experiment and the simulation show that the trapping and the acceleration of electrons in the SM-LWFA is a highly nonlinear process strongly dependent on the wakefield amplitude.

The authors would like to thank M. Baine, K. Evans, and L. Daniels for technical assistance. This work was supported by the Department of Energy and the Office of Naval Research.

*Permanent address: Omega-P, Inc., New Haven, CT 06520.
†Permanent address: Laboratory of Plasma Studies, Cornell University, Ithaca, NY 14853.
‡Permanent address: ICARUS Research, Inc., Bethesda, MD 20824-0780.
§Permanent address: Research Support Instruments Inc., Alexandria, VA 22314.

[1] E. Esarey, P. Sprangle, J. Krall, and A. Ting, IEEE Trans. Plasma Sci. **24**, 252 (1996).
[2] J. A. Edighoffer and R. H. Pantell, J. Appl. Phys. **50**, 6120 (1979); E. Esarey, P. Sprangle, and J. Krall, Phys. Rev. E **52**, 5443 (1995); Y. C. Huang and R. L. Byer, Appl. Phys. Lett. **69**, 2175 (1996); B. Hafizi, A. Ting, E. Esarey, P. Sprangle, and J. Krall, Phys. Rev. E **55**, 5924 (1997).
[3] T. Tajima and J. M. Dawson, Phys. Rev. Lett. **43**, 267 (1979).
[4] C. Clayton *et al.*, Phys. Rev. Lett. **70**, 37 (1993); F. Amiranoff *et al.*, IEEE Trans. Plasma Sci. **24**, 296 (1996).
[5] P. Sprangle, E. Esarey, A. Ting, and G. Joyce, Appl. Phys. Lett. **53**, 2146 (1988).
[6] P. Sprangle, E. Esarey, J. Krall, and G. Joyce, Phys. Rev. Lett. **69**, 2200 (1992); J. Krall, A. Ting, E. Esarey, P. Sprangle, and G. Joyce, Phys. Rev. E **48**, 2157 (1993).
[7] K. Nakajima *et al.*, Phys. Rev. Lett. **74**, 4428 (1995); C. Coverdale *et al.*, Phys. Rev. Lett. **74**, 4659 (1995); D. Umstadter *et al.*, Science **273**, 472 (1996).
[8] A. Modena *et al.*, Nature (London) **337**, 606 (1996); C. E. Clayton *et al.*, Bull. Am. Phys. Soc. **41**, 1465 (1996).
[9] A. Ting, K. Krushelnick, C. I. Moore, H. R. Burris, E. Esarey, J. Krall, and P. Sprangle, Phys. Rev. Lett. **77**, 5377 (1996); S. P. LeBlanc *et al.*, Phys. Rev. Lett. **77**, 5381 (1996).
[10] E. Esarey, J. Krall, and P. Sprangle, Phys. Rev. Lett. **72**, 2887 (1994); W. B. Mori *et al.*, Phys. Rev. Lett. **72**, 1482 (1994); N. E. Andreev *et al.*, Phys. Plasma **2**, 2573 (1995).
[11] A. I. Akhiezer and R. V. Polovin, Zh. Eksp. Teor. Fiz. **30**, 915 (1956) [Sov. Phys. JETP **3**, 696 (1956)].
[12] K. Krushelnick, A. Ting, C. I. Moore, H. R. Burris, E. Esarey, P. Sprangle, and M. Baine, Phys. Rev. Lett. **78**, 4047 (1997).
[13] D. Umstadter *et al.*, Phys. Rev. Lett. **59**, 292 (1987).
[14] J. R. Marques *et al.*, Phys. Rev. Lett. **76**, 3566 (1996).
[15] K. Krushelnick, A. Ting, C. I. Moore, and H. R. Burris, "Large Amplitude Radial Plasma Wave Generation during High Intensity Laser Interaction with Underdense Plasmas" (to be published).
[16] A. Ting, K. Krushelnick, H. R. Burris, A. Fisher, C. Manka, and C. I. Moore, Opt. Lett. **21**, 1096 (1996).
[17] P. Bertrand *et al.*, Phys. Rev. E **49**, 5656 (1994).
[18] E. Esarey and P. Sprangle, Phys. Rev. A **45**, 5872 (1992); G. Shvets *et al.*, Phys. Plasmas **4**, 1872 (1997).
[19] E. Esarey, R. F. Hubbard, W. P. Leemans, A. Ting, and P. Sprangle, Phys. Rev. Lett. **79**, 2682 (1997).